

## Magnetotransport in two-dimensional lateral superlattices

Axel Lorke and Jörg P. Kotthaus

*Sektion Physik, Universität München, Geschwister-Scholl-Platz 1, 8000 München 22, Germany*

Klaus Ploog

*Max-Planck-Institut für Festkörperforschung, Heisenbergstrasse 1, 7000 Stuttgart 80, Germany*

(Received 12 February 1991)

Two-dimensional electron systems on GaAs heterostructures subjected to a two-dimensional superlattice potential reveal novel features in the magnetoresistance. Strong density modulation causing the formation of antidots is accompanied by a pronounced magnetoresistance maximum. On weakly modulated systems, oscillations are observed that reflect the commensurability of the cyclotron diameter and the superlattice period. A classical model of ballistic motion resulting in magnetic-field-dependent diffusion is found to explain our and other recent magnetotransport observations.

Advances in micropatterning of two-dimensional electron systems at semiconductor interfaces have rendered it possible to fabricate lateral two-dimensional (2D) superlattices with periodicities down to about 200 nm. Initial experiments performed on such systems have concentrated on the study of isolated electron dots.<sup>1-7</sup> Recently, the scope has been extended to lateral superlattice phenomena in periodically modulated two-dimensional electron gases.<sup>7-18</sup> A special feature of these systems is the fact that the electric forces of the confining potential can be comparable to the magnetic forces acting upon the electrons even at moderate magnetic fields. Already at weak superlattice modulation, this yields novel structures in the static magnetoconductivity.<sup>8-14</sup> A complementary structure to a dot array, i.e., a so-called "antidot" array can be obtained by inducing an array of voids in a formerly two-dimensional electron gas.<sup>15-18</sup> Such a structure can be considered the solid-state realization of a Sinai billiard. Chaotic conductance fluctuations, anomalous diffusion, and  $1/f$  noise have been predicted for these systems.<sup>19,20</sup>

Here we present magnetotransport studies of 2D lateral superlattices that can be gate-voltage tuned from moderate density modulation to the formation of antidots. On antidot arrays we observe a strong magnetoresistance maximum when the cyclotron diameter approximately equals the superlattice period. On moderately modulated superlattices we observe oscillations reflecting the commensurability between the cyclotron diameter and the superlattice period. Both phenomena and their observed dependence on applied gate bias are explained by introducing a semiclassical diffusion model based on ballistic transport in a 2D superlattice potential under the influence of the Lorentz force. Comparison with other experimental results leads us to conclude that such a simple model is able to explain many essential features of magnetotransport so far observed in 2D lateral superlattices.

The preparation of our 2D superlattices starts from high-mobility GaAs-Ga<sub>1-x</sub>Al<sub>x</sub>As heterostructures grown by molecular-beam epitaxy. A Hall bar of 1.5 mm length and 100  $\mu$ m width is defined through a wet etching process. Small pads of InAg alloy are diffused into the current and voltage leads to provide Ohmic contacts. The samples are then covered with photoresist that is double

exposed by an interference grating using standard holographic techniques.<sup>7</sup> Developing removes the photoresist in the areas of strongest exposure so that an array (grating constant  $a=460$  nm) of voids ( $\approx 170$  nm radius) is formed in the photoresist. The resist is then covered by a thin Ni-Cr layer to serve as a modulated gate. A voltage applied to the gate electrode provides the tunable 2D superlattice potential. An antidot lattice is formed under sufficiently high negative bias such that the areas beneath the voids in the photoresist become fully depleted.<sup>15</sup>

Characteristic magnetoresistance traces of antidot superlattices are displayed in Fig. 1 for two different samples. For sample *A* with a low electron density  $N_s$  (trace *a*) the resistance peak appears at a magnetic field of  $B=0.23$  T. Sample *B* with a relatively high density exhibits a maximum at a somewhat higher magnetic field of 0.33 T (trace *b*). After increasing  $N_s$  in sample *B* through infrared illumination the maximum shifts to an even higher magnetic field of 0.54 T (trace *c*). Apart from its clear dependence on the electron density, the position of the magnetoresistance peak is quite insensitive to many experimental parameters such as temperature (in the range between 1.8 and 4.2 K), measuring current, and measuring geometry (two or four terminal, along or across the Hall bar). However, it only appears at sufficiently negative gate voltages close to or below the threshold at which the antidot lattice is formed. The formation of the antidot lattice is monitored by a dramatic decrease in the gate capacitance with decreasing gate voltage. Before this takes place all commensurability oscillations (see below) have vanished and the resistance maximum develops out of a basically featureless low-field magnetoresistance (dotted line in Fig. 1).

In a naive picture we have checked whether the prominent magnetoresistance maximum can be understood as magnetic-field-induced crystallization of the electrons onto the antidot lattice. Calculating the classical cyclotron diameter  $2R_c$  for electrons at the Fermi energy from the measured electron density  $N_s$  via

$$2R_c = 2 \frac{\hbar}{eB} (2\pi N_s)^{1/2}, \quad (1)$$

we derive 490, 570, and 470 nm at maximum resistance

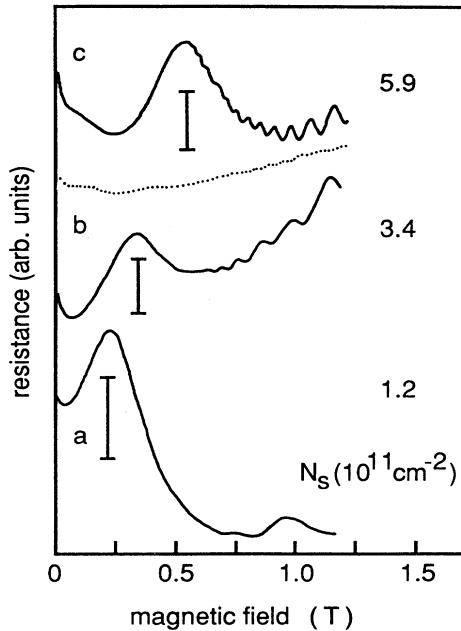


FIG. 1. Magnetoresistance of different electrostatically defined antidot arrays of period  $a=460$  nm. Below the onset of Shubnikov-de Haas oscillations a prominent maximum in the resistance appears, shifting to higher magnetic fields with increasing electron density  $N_s$ . The gate voltages are sufficiently negative to induce an antidot superlattice ( $-0.27$  V,  $-0.42$  V, and  $-0.90$  V for traces *a*, *b*, and *c*, respectively). The dotted line gives the magnetoresistance *c* before antidot formation ( $V_g = -0.8$  V). The electron densities  $N_s$  given are determined from the Shubnikov-de Haas oscillations. Bars correspond to 10% of the zero-field resistance.

for the traces *a*, *b*, and *c*, respectively, of Fig. 1. This is in close agreement with the grating constant of the antidot array  $a=460$  nm. In a picture of magnetic crystallization the magnetic field directs the electrons at the Fermi energy on rather stable orbits around the antidots whenever  $2R_c \approx a$ . This way the electrons become localized which reduces charge transport and causes the magnetoresistance maximum.

For a more quantitative model of magnetotransport in a 2D superlattice we numerically calculate the classical trajectories of electrons at constant Fermi energy  $E_F$  above the minima of the subband edge in a 2D periodic potential under the influence of a magnetic field. Following the billiard model approach by Beenakker and van Houten,<sup>21,22</sup> we compute the mean-squared distance  $r^2$  that a set of electrons (typically 3000) with initial spatial and momentum coordinates chosen at random covers in an average time  $\tau$ . Here  $\tau=24$  ps represents the momentum scattering time corresponding to the mobility of the unmodulated two-dimensional electron gas of typically  $600000$  cm<sup>2</sup>/V s. We then calculate the two-dimensional diffusion constant

$$D = \frac{r^2}{4\tau} \quad (2)$$

and derive the resistivity  $\rho$  using the Einstein relation,

$\rho = 1/DNe^2$ , with  $N = m/\pi\hbar^2$  being the density of states of a two-dimensional electron gas. Figure 2(a) shows the calculated mean-squared distance  $r^2$  as a function of magnetic field. For simplicity we approximated the periodic potential by

$$V(x,y) = V_0[\cos(kx) + \cos(ky) + 2], \quad k = \frac{2\pi}{a}. \quad (3)$$

In Fig. 2, a Fermi energy of  $E_F = 9$  meV accounts for an electron density of  $2.6 \times 10^{11}$  cm<sup>-2</sup>. The Fourier coefficient  $V_0 = 4$  meV was chosen such that we have well-defined narrow constrictions between the antidots with a sufficiently high transmission probability for electrons at the Fermi energy. At  $B = 0.3$  T a minimum in  $r^2$  becomes apparent reflecting that at this field the diffusion is suppressed by the localization of the electrons to the antidot lattice. This becomes even more obvious in Fig. 2(b) where  $\rho$  is plotted versus  $B$ . The peak magnetic field of 0.3 T and the Fermi energy of 9 meV correspond to a classical cyclotron diameter of 560 nm which is, as for the experimental data, slightly larger than the periodicity  $a = 460$  nm of the antidot lattice. The resistance peak can also be related to the magnetotransport anomalies observed in mesoscopic multiprobe conductors.<sup>22,23</sup> Then the effect of the antidot array may be understood as that of a lattice of microscopic Hall bars as depicted in the inset of Fig. 2. The resistances of the individual Hall bars exhibiting a maximum at low magnetic fields add up to the macroscopic sheet resistance measured in our samples.

Figure 3 shows the measured four-point magnetoresistance  $R_{xx}$  of sample *B* with positive gate bias. Below the onset of Shubnikov-de Haas oscillations strong additional

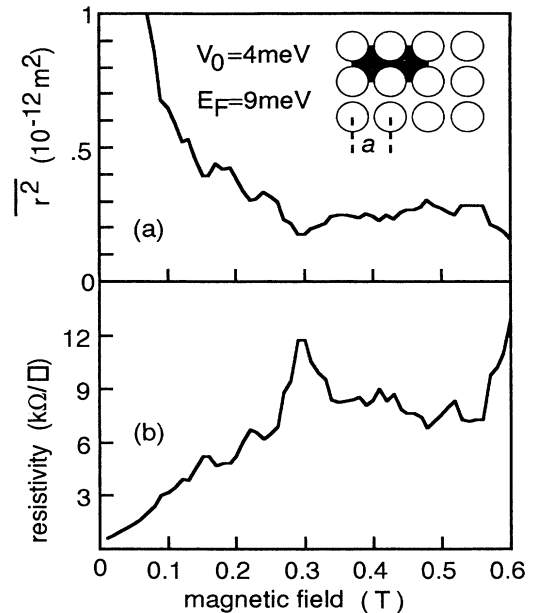


FIG. 2. Simulated transport through an antidot lattice of period  $a=460$  nm. (a) Mean-squared distance covered by electrons in an average time  $\tau=24$  ps. (b) Resistivity calculated from (a). At 0.3 T a maximum is observed due to reduced diffusion.

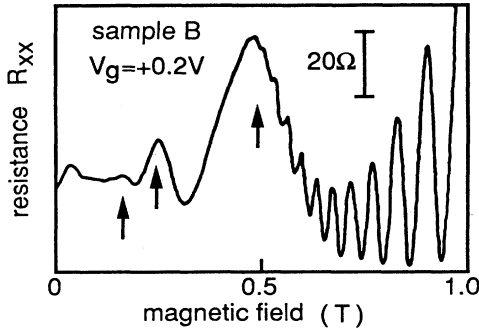


FIG. 3. Measured magnetoresistance of sample *B* under positive bias. Commensurability oscillations (arrows) are observed. Shubnikov-de Haas oscillations appear above 0.5 T. The electron density is  $N_s = 5.7 \times 10^{11} \text{ cm}^{-2}$ . The resistance at  $B = 0$  is  $R_{xx} = 350 \Omega$ .

magnetoresistance oscillations are observed (arrows). These oscillations that are periodic in  $1/B$  are well known from 1D modulated lateral superlattices<sup>8</sup> and can either be explained in a quantum-mechanical picture of Landau band formation<sup>9,10</sup> or in a classical picture of a magnetic-field-dependent guiding center drift.<sup>21</sup> For the resistance across the 1D superlattice grating ( $R_{xx}$ ) they are now understood to be of predominantly classical origin and to reflect oscillations of the net drift velocity. Weak anti-phase oscillations observed in  $R_{yy}$ , however, are explained as quantum oscillations of the scattering rate.<sup>24</sup> In the case of 1D modulation, maxima in the resistance  $R_{xx}$  are expected whenever the relation

$$2R_c = (m + \phi)a, \quad m = 1, 2, \dots, \quad \phi = 0.25 \quad (4)$$

is satisfied. For the 2D case it has not yet been clarified whether the oscillations observed by various groups on different sample configurations<sup>11-14</sup> are of predominantly classical or quantum-mechanical origin. Also, varying phase factors  $\phi$  have been observed in the different experiments.<sup>11-14</sup> The only model proposed so far explains the oscillations as being of quantum-mechanical origin.<sup>25</sup> In the following we want to show that our simple classical model seems to be able to account for all essential observations reported so far for lateral 2D superlattices.

In order to extend our model to the case of weak modulation we can no longer neglect the off-diagonal components of the diffusion tensor  $\bar{D}$  and the conductivity tensor  $\bar{\sigma}$  as it was safely done for the antidot lattice above.<sup>26</sup> Generally, a weak laterally periodic potential mainly affects the diagonal components of  $\bar{\sigma}$  and  $\bar{D}$ .<sup>21</sup> When the cyclotron frequency  $\omega_c \gg 1/\tau$  the large off-diagonal terms cause maxima in  $R_{xx}$  to correspond to maxima in  $\sigma_{yy}$ . The relative change in resistance caused by the superlattice potential can then be obtained from

$$\frac{R_{xx}}{R_{xx0}} = \frac{D}{D_0} = r^{-2} \frac{1 + (\omega_c \tau)^2}{2(v_F \tau)^2}. \quad (5)$$

Here  $D$  is the diffusion constant obtained from the quasi-classical simulations and  $D_0 = \frac{1}{2} v_F^2 \tau / [1 + (\omega_c \tau)^2]$  the

diffusion constant in the unperturbed case with  $v_F$  being the Fermi velocity.

Figure 4(a) gives the calculated ratio  $D/D_0$  as a function of the magnetic field. Oscillations appear (arrows) with maxima that are linear in  $1/B$  as in Eq. (4) with  $\phi = -0.25$ . This is consistent with data obtained experimentally for persistent photo-effect-induced electron-density modulation.<sup>14</sup> Our data shown in Fig. 3, however, yield a value  $\phi = 0$ . This phase difference can be attributed to that the potential of Eq. (3), leading to the result  $\phi = -0.25$ , does not adequately describe the potential of our antidot sample under positive bias. To achieve a more realistic potential we have added a cross term in the Fourier expansion of the potential

$$V(x, y) = V_0 [\cos(kx) + \cos(ky) - \cos(kx)\cos(ky) + 3]. \quad (6)$$

This potential, depicted in the inset of Fig. 4(b), also yields oscillations but with a phase  $\phi = 0$ , in agreement with the experimental data of Fig. 3.

The above calculations show beyond doubt that also for a 2D potential modulation the commensurability oscillations can be explained within a classical model of diffusive transport through the lateral superlattice. Unlike in the one-dimensional case the exact shape of the potential is of considerable importance for the exact value of the phase  $\phi$ .

In conclusion, we have studied the magnetoresistance of antidot arrays and lateral 2D superlattices. On antidot lattices we observe a pronounced magnetoresistance maximum shifting to higher magnetic fields with increasing electron density. Within a classical billiard model it is ex-

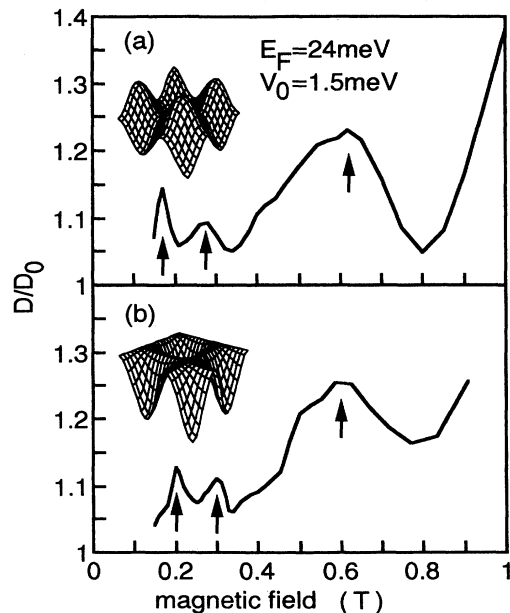


FIG. 4. Calculated commensurability oscillations for different shapes of the potential as sketched in the insets. A shift in the phase  $\phi$  from (a)  $-0.25$  to (b)  $0$  is evident.

plained as reduced diffusion caused by electron crystallization onto the antidot lattice due to the interplay of magnetic and electric forces when the cyclotron diameter approximately equals the lattice constant. Under positive bias we observe commensurability oscillations linear in  $1/B$ . By simulating the transport through weakly modulated 2D periodic potentials we are able to explain these oscillations within a classical picture of diffusive transport. The simulations demonstrate that a cross term in the expansion of the potential can change the phase shift  $\phi$

of the commensurability oscillations which renders it difficult to unambiguously identify  $\phi$  experimentally.

We would like to thank C. W. J. Beenakker, R. W. Winkler, and J. Alsmeier for many stimulating discussions contributing to the ideas presented in this paper. Financial support by the ESPRIT (European Strategic Programme of Research and Development in Information Technology) Basic Research action is gratefully acknowledged.

- 
- <sup>1</sup>T. P. Smith III, K. Y. Lee, C. M. Knodler, J. M. Hong, and D. P. Kern, *Phys. Rev. B* **38**, 2172 (1988).
- <sup>2</sup>M. A. Reed, J. N. Randall, R. J. Aggarwal, R. J. Matyi, T. M. Moore, and A. E. Wetsel, *Phys. Rev. Lett.* **60**, 535 (1988).
- <sup>3</sup>Ch. Sikorski and U. Merkt, *Phys. Rev. Lett.* **62**, 2164 (1989).
- <sup>4</sup>W. Hansen, T. P. Smith III, K. Y. Lee, J. A. Brum, C. M. Knodler, J. M. Hong, and D. P. Kern, *Phys. Rev. Lett.* **62**, 2168 (1989).
- <sup>5</sup>J. Alsmeier, E. Batke, and J. P. Kotthaus, *Phys. Rev. B* **41**, 1699 (1990).
- <sup>6</sup>T. Demel, D. Heitmann, P. Grambow, and K. Ploog, *Phys. Rev. Lett.* **64**, 788 (1990).
- <sup>7</sup>A. Lorke, J. P. Kotthaus, and K. Ploog, *Phys. Rev. Lett.* **64**, 2559 (1990).
- <sup>8</sup>D. Weiss, K. von Klitzing, K. Ploog, and G. Weimann, *Europhys. Lett.* **8**, 179 (1989).
- <sup>9</sup>R. W. Winkler, J. P. Kotthaus, and K. Ploog, *Phys. Rev. Lett.* **62**, 1177 (1989).
- <sup>10</sup>R. R. Gerhardts, D. Weiss, and K. von Klitzing, *Phys. Rev. Lett.* **62**, 1173 (1989).
- <sup>11</sup>P. H. Beton, E. S. Alves, M. Henini, L. Eaves, P. C. Main, O. H. Hughes, G. A. Toombs, S. P. Beaumont, and C. D. W. Wilkinson, *J. Phys. Condens. Matter* **1**, 8257 (1989).
- <sup>12</sup>K. Ismail, T. P. Smith III, and W. T. Masselink, *Appl. Phys. Lett.* **55**, 2766 (1989).
- <sup>13</sup>H. Fang and P. J. Stiles, *Phys. Rev. B* **41**, 10171 (1990).
- <sup>14</sup>D. Weiss, K. von Klitzing, K. Ploog, and G. Weimann, *Surf. Sci.* **229**, 88 (1990).
- <sup>15</sup>A. Lorke, J. P. Kotthaus, and K. Ploog, *Superlattices Microstruct.* **9**, 103 (1991).
- <sup>16</sup>K. Ensslin and P. M. Petroff, *Phys. Rev. B* **41**, 12307 (1990).
- <sup>17</sup>K. Kern, D. Heitmann, P. Grambow, Y. H. Zhang, and K. Ploog, *Phys. Rev. Lett.* **66**, 1618 (1991).
- <sup>18</sup>D. Weiss, M. L. Roukes, A. Menschig, P. Grambow, K. von Klitzing, and G. Weimann, *Phys. Rev. Lett.* **66**, 2790 (1991).
- <sup>19</sup>R. A. Jalabert, H. U. Baranger, and A. D. Stone, *Phys. Rev. Lett.* **65**, 2442 (1990).
- <sup>20</sup>T. Geisel, J. Wagenhuber, P. Niebauer, and G. Obermair, *Phys. Rev. Lett.* **64**, 1581 (1990).
- <sup>21</sup>C. W. J. Beenakker, *Phys. Rev. Lett.* **62**, 2020 (1989).
- <sup>22</sup>C. W. J. Beenakker and H. van Houten, *Phys. Rev. Lett.* **63**, 1857 (1989).
- <sup>23</sup>M. L. Roukes, A. Scherer, S. J. Allen, Jr., H. G. Craighead, R. M. Ruthen, E. D. Beebe, and J. P. Harbison, *Phys. Rev. Lett.* **59**, 3011 (1987).
- <sup>24</sup>C. Zhang and R. R. Gerhardts, *Phys. Rev. B* **41**, 12850 (1990).
- <sup>25</sup>R. R. Gerhardts, D. Weiss, and U. Wulf, *Phys. Rev. B* **43**, 5192 (1991).
- <sup>26</sup>For antidot lattices both the experimental and the computational data show negligible Hall drift and Hall voltage.